Contract No.:

This manuscript has been authored by Savannah River Nuclear Solutions (SRNS), LLC under Contract No. DE-AC09-08SR22470 with the U.S. Department of Energy (DOE) Office of Environmental Management (EM).

Properties of $Cd_{0.90-x}Mn_xZn_{0.10}Te$ (x = 0.10, 0.20) crystals grown by Vertical Bridgman method

V. Kopach[1], O. Kopach[1], A. Kanak[1], L. Shcherbak[1], P. Fochuk[1], A. E. Bolotnikov[2], R. B. James[3]
[1] – Chernivtsi National University, Ukraine
[2] – Brookhaven National Laboratory, USA
[3] – Savannah River National Laboratory, USA

ABSTRACT

The correlation between $Cd_{0.90-x}Mn_xZn_{0.10}Te$ (CMZT) melt state and structural properties of the crystals, grown by vertical Bridgman method, was investigated. The $Cd_{0.9-x}Mn_xZn_{0.1}Te$ crystals with various Mn compositions (x = 0.1 and 0.2) were grown by a two-step method from high-purity elemental components. We have conducted a series of crystal growth runs with different degrees of melt superheating over the alloy's melting temperature. We obtained ingots with various crystalline structures and properties. It was concluded that the best crystals were grown from the melt with a thermal gradient of about 5 °C/cm during growth process. We have found that the band-gap increases (from 1.67 eV at x=0.1 to 1.79 eV at x=0.2) with Mn content.

Keywords*:* semi-magnetic semiconductor, CMZT, Bridgman technique, single crystal growth, growth from melt.

1. INTRODUCTION

Vertical Bridgman (VB) method is the one of the most convenient and commonly used methods for growing single-crystals compounds based on CdTe [1]. However, one of the main difficulties of this method is to maintain a small temperature gradient to avoid supercooling in the melt, which can lead to uncontrolled nucleation and fast growth, and consequently, single crystals of poor quality. As a result, the grown ingot has a different composition along its length. Furthermore, it can give rise to high crystalline defects, such as sub-grain boundaries, dislocations, Te inclusions, etc. Thus, it's important to study the growth process to improve single crystal structure.

In the past, the diluted magnetic semiconductors $Cd_{1-x-y}Mn_xZn_yTe$ attracted attention of researchers due to their magneto-optical properties, the band-gap width, Faraday rotation [2, 3] and ferromagnetism in $Cd_{1-y}Mn_{0.35}Zn_yTe$ single crystals [4]. Until now CMZT crystals were grown by a VB method [1-3] and the temperature-gradient solution method [4]. However, in these studies, no information was available regarding the liquidus-solidus temperatures in the composition range for the $Cd_{1-x-y}Mn_xZn_yTe$ solid solutions [2-4] beyond a diagram for the $Cd_{1-x-y}Mn_xZn_yTe$ pseudo-ternary alloys [1] showing the concentration dependencies for constant lattice parameters.

Here we present experimental evidence of the effects of the melts superheating in the VB growth of $Cd_{0.9-x}Mn_xZn_{0.1}Te$ crystals due to the modifications of the growth process based on the DTA results shown in [5-7].

2. EXPERIMENTS

2.1 Synthesis of the $Cd_{0.9-x}Mn_xZn_{0.1}Te$ alloys

Synthesis of the $Cd_{0.9-x}Mn_xZn_{0.1}Te$ (x=0.1 and 0.2) alloys was carried out in a vertical furnace. To prevent the possibility of Mn interaction with the quartz crucible walls, a glassy carbon crucible was used. Due to the selected temperature gradient, sublimation of the components was excluded during the synthesis.

The total weight of the experimental samples was about 40 g. High-purity starting elements Cd, Zn, Mn and Te were loaded in the glassy carbon crucible in a certain order. Then, the crucible was loaded inside the quartz ampoule and evacuated to $4x10^{-4}$ mbar. The ampoule was placed inside a two-zone furnace for melting of the charge and held for 24 hours at a maximal temperature before turning to pre-programmed cooling. Two thermocouples were placed inside the cartridge along the ampoule to monitor the temperatures.

2.2 Crystal growth

The polycrystalline CMZT was loaded into the carbon-coated quartz ampoule and sealed under a vacuum of 3.4×10^{-4} mbar at room temperature. The conical tip of the ampoule was designed to promote spontaneous nucleation. A custom-designed, two-zone vertical Bridgman furnace was used. A computer-controlled thermal profile inside the furnace is shown in Fig. 1. For monitoring the temperature, a thermocouple was placed at the bottom of the ampoule. As seen in Fig. 1, the temperatures at the top of the ampoule (T_2) were higher than at the bottom (T_1).

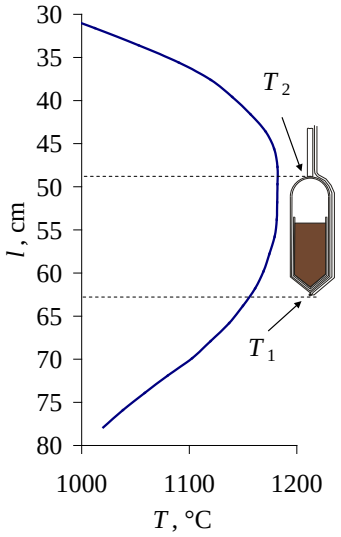

Figure 1. Temperature profile and ampoule position inside the growth furnace.

The ampoule movements with the attached thermocouples were controlled by a PC. The sample composition and growth parameters for all growth ingots are summarized in Table 1.

Using a different thermal analysis, we found previously that the melting temperature of the $Cd_{0.9-x}Mn_xZn_{0.1}Te$ (x=0.1 and 0.2) polycrystalline materials is 1096-1098 C, while the freezing temperature is 1085-1089 °C [6]. The synthesized samples were heated up to about 980 °C in 7 h, and then their temperatures were slowly raised to the dwell temperature over 2 h and maintained at this level for about 30 h. The temperature of the bottom of the ampoule was raised up to 1132 °C (for the CMZT-1 growth process), 45 °C higher than the $Cd_{0.8}Mn_{0.1}Zn_{0.1}Te$ melting point, to ensure that the polycrystalline material was completely melted. The hot zone provided a maximum temperature of 1165 °C, and the cold zone was kept about 1132 °C to control the growth process and to determine the thermal gradient of about 10 °C/cm. The ampoule was pulled down with a rate of 2.7 mm/h. After lowering the ampoule to a certain length, the cooling procedure was turned on to reduce the thermal stresses of the grown crystal.

Table 1. Samples composition and growth parameters for the ingots

Sample	x in $Cd_{0.9-x}Mn_xZn_{0.1}Te$	mass, g	Growth temperature, °C (bottom of the ampoule)	Thermal gradient, °C/cm
CMZT-1	0.10	39	1132	9.9
CMZT-2	0.10	34	1142	6.4
CMZT-3	0.20	33	1139	4.4
CMZT-4	0.20	39	1149	3.7

The procedure for growing CMZT crystals is described below:

1. The starting elements Cd, Zn, Mn and Te were loaded in the glassy carbon crucible in a certain sequence.
2. The growth ampoule was positioned along the thermal profile inside the furnace such that the sample would be completely melted when the furnace temperature settings were reached.
3. The growth temperature was determined by DTA experiments, which were described in our previous papers [5-7].

4. Different values for the thermal growth gradient were used.

The obtained crystals were about 40 mm in length. For further studies, the crystals were sliced by a wire saw into 2-mm-thick pieces, then polished by $A1_2O_3$ powder and 5% bromine-methanol solution. The as-grown ingots were characterized and studied.

Optical analysis was performed using a transmission method with an Ocean Optics OO-2000 Spectrometer. For detecting precipitates and inclusions, we used IR transmission microscopy (Leitz) with the camera PixeLINK PL-A741 ($\lambda \sim 1$ μm). High temperature electrical measurements (HTEM) were conducting by the six-contact method using the measurement equipment described in [8].

3. RESULTS AND DISCUSSIONS

3.1 Polycrystalline materials

The initial charge in the ampoule was heated for ~ 9 hours to the maximal dwell temperature (Fig. 2). During heating two exothermal effects were recorded. According to the experimental values, the first reaction temperature is observed at 450±4 °C for all materials, which corresponds to the Te melting temperature (449.6 °C). The next exothermic effect, which occurs in a wider temperature interval from 780 to 920 °C, can be explained by the boiling of Cadmium (767 °C), Zinc (907 °C) and Tellurium (988 °C). After reaching the maximal temperatures, the necessary temperatures were adjusted. To protect the vaporization of volatile components, the temperature at the top of the ampoule (T_2) was held at level of 30-40 °C higher than the temperature at the ampoule's bottom (T_1). As can be seen from Fig. 2, the exothermic

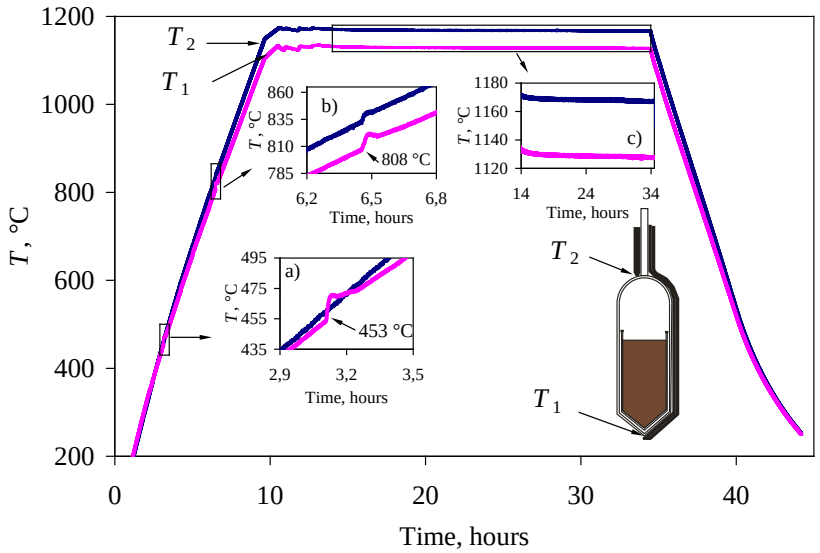

Figure 2. The temperature profile for CMZT-2 synthesis. The inserts show exothermal effects during synthesis (a, b), the temperatures during the melt holding, (c) and the thermocouples positions in the ampoule.

effects during the synthesis of CMZT-2 bulk occur at 453 °C and 808 °C. Here, the melt was held for at least 20 hours in the programmed temperature gradient from 1130±1 °C (T_1, bottom of the ampoule) to 1170 ±1 °C (T_2, top of the ampoule). The synthesized charge cooling was performed over 10 -12 hours.

3.2 Single crystals

As seen from Table 1, the CMZT-1 and CMZT-2 crystals have the same composition (x=0.1), but the thermal gradient during the growth process was different (9.9 and 6.4 °C/cm for CMZT-1 and CMZT-2, respectively, see Fig. 3 curves 1 and 2). CMZT-3 and CMZT-4 ingots (x=0.2) were grown similarly with thermal gradients of 4.4 and 3.7 °C/cm, respectively (Fig. 3, curves 3 and 4). The goal of this experiment was to investigate the influence of the thermal gradient on crystal quality.

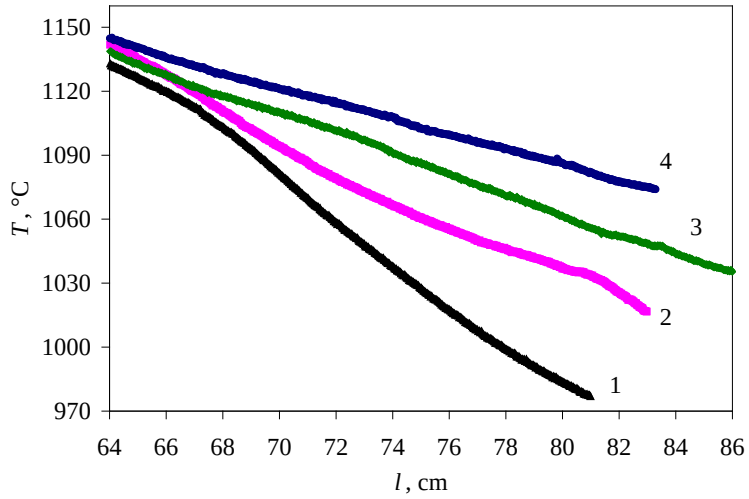

Figure 3. Temperature vs. position in the furnace during crystal growth: 1 – CMZT-1, 2 – CMZT-2, 3 – CMZT-3, 4 – CMZT-4.

Figs. 4 and 5 show images of CMZT-1 and CMZT-2 ingots, respectively. CMZT-1 ingot (Fig. 4a) has some cavities and pores, while CMZT-2 (Fig. 5a) has a smooth surface. We suppose that the higher growth temperature supports better homogenization of the polycrystalline material and as a result better crystal structure. A photograph of the CMZT-1 wafer (Fig. 4a) demonstrates good crystallinity with some monocrystalline grains. Meanwhile, the ingot CMZT-2 has only two monocrystalline grains (Fig. 5c).

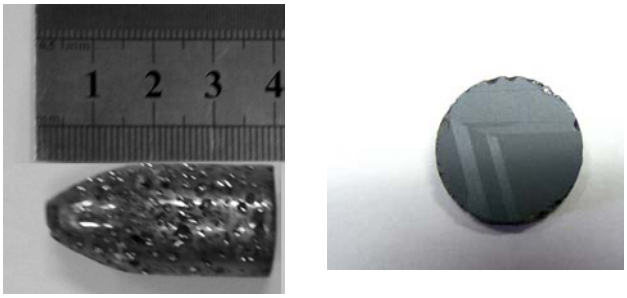

a) b)

Figure 4. As-grown CMZT-1 ingot (a) and wafer with multiple grains (b).

a) b)

Figure 5. The first-to-freeze part of as-grown ingot CMZT-2 (a) wafer with two monocrystalline areas (b).

The structure of the other ingots CMZT-3 and CMZT-4 with x = 0.2 have some peculiarities. It is well-known that the CMT crystals with Mn content of 20-30 mol % are prone to formation of twins during the growth process [9, 10]. In this work, the tendency to form twins within the grown crystals was also observed. Thus, the twins in the ingot CMZT-3

were found along the whole wafer (Fig. 6b), while the as-grown crystal CMZT-4 has polycrystalline structure composed of small grains, and some of them have twinning. Perhaps the overheating of our sample during the growth process by about 10 °C leads to a decrease in the ability to form twins and monocrystalline domains.

a) b)

Figure 6. As-grown ingot CMZT-3 (a), the wafer from the CMZT-3 crystal with twins (b).

a) b)

Figure 7. As-grown crystal CMZT-4 (a), the multiple grains in CMZT-4 sample with twins (b).

Fig. 8 shows typical IR microscope images for different as-grown CMZT slices. As we can see, the size of the Te inclusions is about 5-20 μm in all samples. However, the Te inclusions in the ingots CMZT-3 and CMZT-4 are distributed more uniformly across the entire plane of the crystals, while the ingots CMZT-1 and CMZT-2 have Te inclusions predominantly along certain areas across the crystal.

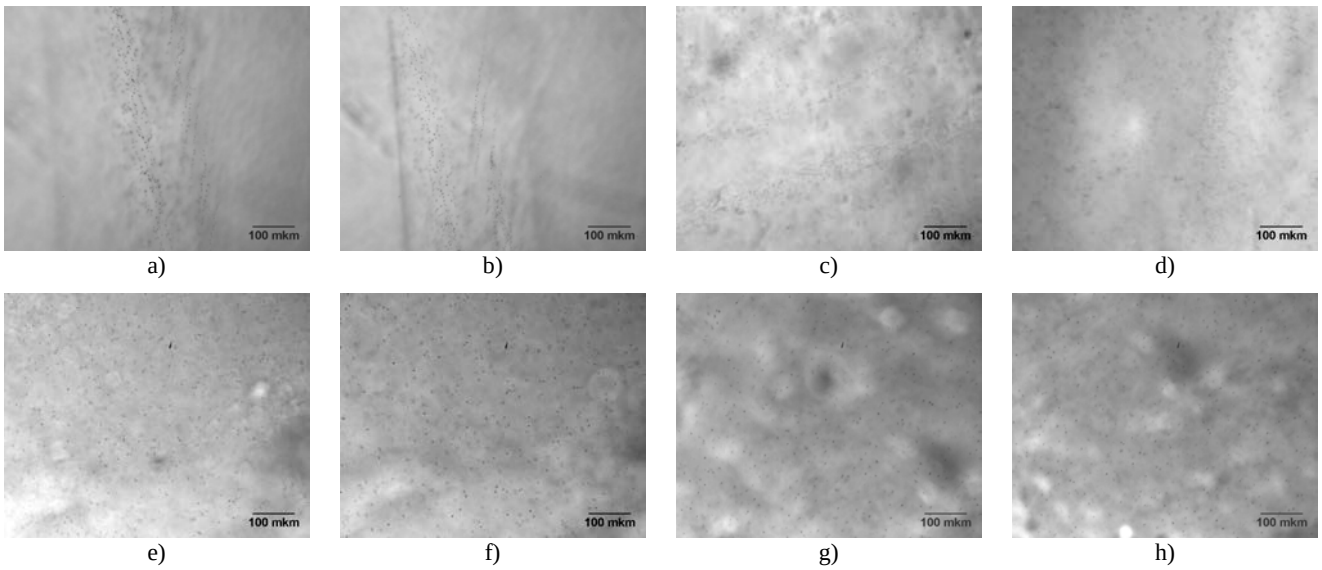

a) b) c) d)

e) f) g) h)

Figure 8. IR images of as-grown CMZT-1 (a,b), CMZT-2 (c,d), CMZT-3 (e,f) and CMZT-4 (g,h) crystals.

Fig. 9 shows typical transmission spectra for as-grown CMZT-1, CMZT-2, CMZT-3 and CMZT-4 crystals. As we can see the highest transmission is at about 65 % for the CMZT-2 crystal, which has good crystalline structure and consists of two monocrystalline grains. CMZT-4 crystal has a polycrystalline structure composed of small grains with a

twinning structure; it possesses a very low transmission value of about 32 %. The low transmission values of CMZT-3 and CMZT-4 ingots are caused by the relatively high amount of Te inclusions in these crystals.

The sample's band-gap rises from 1.67 eV at x=0.1 to 1.79 eV at x=0.2, i.e. with increasing Mn content. Based on the data from our previous work [7], the value of the band-gap for CMZT-1 ($Cd_{0.75}Mn_{0.20}Zn_{0.05}Te$) crystal is about 1.77-1.78 eV, while such values for the CMZT-3 and CMZT-4 crystals ($Cd_{0.70}Mn_{0.20}Zn_{0.10}Te$) are 1.79-1.80 eV. It's evident that increasing the amount of Zn component from 0.05 to 0.10 mol. % leads to an increase in the value of the band-gap for CMZT crystals.

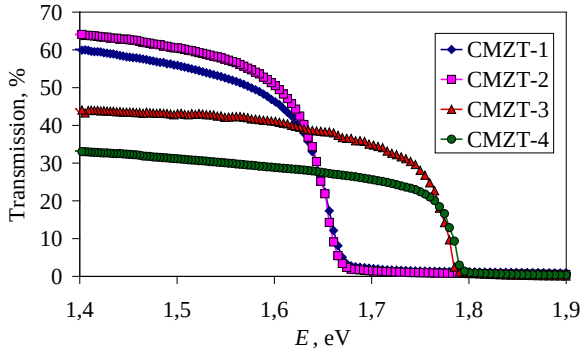

Figure 9. Typical transmission spectrum of as-grown CMZT crystals.

To evaluate the effect of Te inclusions on the electrical parameters of as-grown crystals, the high-temperature electrical characteristics of the samples were measured (Fig. 10, 11). During the conduct of high-temperature measure-

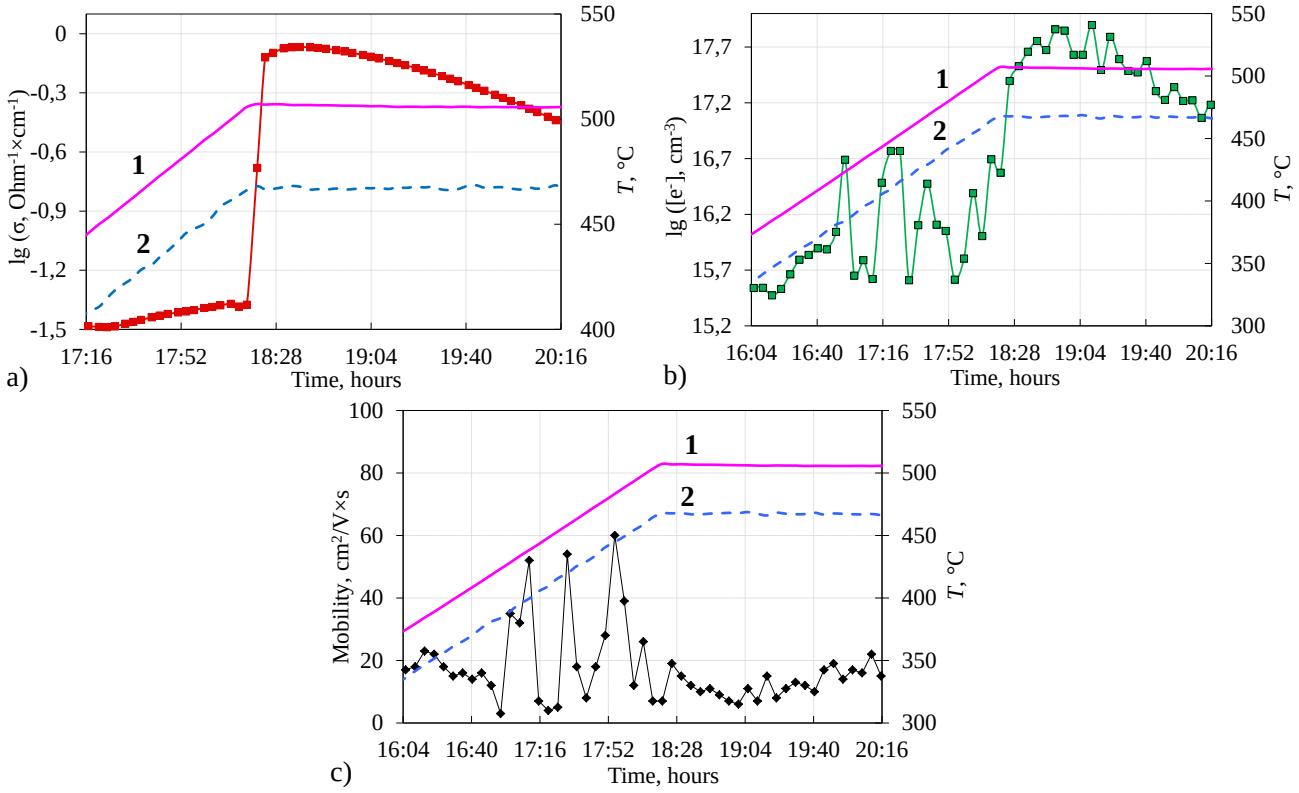

Figure 10. Time-dependence of the electrical conductivity (a), carrier concentration (b), and mobility (c) in the CMZT-1 versus the zone temperature for sample (1) and the component (Cd) (2). 1 - sample temperature; 2 - Cd temperature.

ments of the electrical properties (annealing at ~500 °C), a sharp increase of the electrical conductivity and charge-carrier concentration were measured (Figs. 10 a, b). The oscillation of the carriers' concentration and their mobility occurred before the significant increase of the conductivity, as can be seen from Figs. 10 b, c. A similar electrical conductivity "jump" for CdTe, Cd(Zn)Te and Cd(Mn)Te was associated in [11,12] with melting of the tellurium inclusions. Uncontrolled impurity atoms, which are contained in these inclusions, are ionized and therefore generate additional charge carriers.

At the beginning of the measurements in the range from 300 °C to 500 °C, the concentration of charge carriers in the CMZT-1 sample was ~10^{16} cm^{-3} (Fig. 11a). Due to melting of the tellurium inclusions at ~500 °C, an increase of [e^-] followed by a return to the previous value was recorded. During the next annealing at ~500 °C, a decrease of the electron concentration close to the line expected for the intrinsic carrier concentration in undoped CdTe over a wide temperature

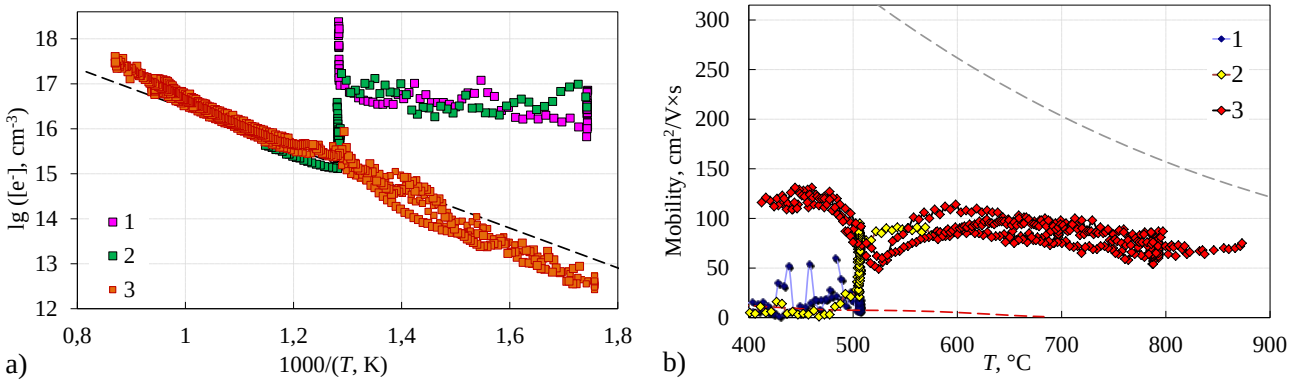

Figure 11. Temperature dependence of concentration (a) and mobility of charge-carriers (b) in CMZT-1 at p_{Cd}, max. The numbers 1,2 and 3 indicate the order of measurements. Dashed line in (a) is intrinsic carrier concentration in undoped CdTe; (b): a modeling for hole mobility (lower line) and electron mobility (upper line) in undoped CdTe.

range (300-900 °C) was observed. In addition, an increase of the mobility of charge carriers from 10-20 cm^2/V-s to 90-120 cm^2/V-s after the second heating to 500 °C (Fig. 11b) was obtained. The minimum of the measured values for the charge-carrier mobility at 530 °C (Fig. 11b) is of additional interest and requires further investigation.

4. CONCLUSION

The correlation between the CMZT melt state and structure properties of crystals grown by the vertical Bridgman method was investigated. We used different thermal gradients for the crystal growth process for ingots with the same composition. We observed that for the growth of CMZT crystals with better crystalline structure, the thermal gradient for the growth process should be about 5 °C/cm. As in our previous work, the value of the crystals band-gap rose with increasing Mn content (from 1.67 at x=0.1 to 1.79 eV at x=0.2). The high-temperature measurement established that the sharp increase in the electrical conductivity, which is inherent for CdTe, Cd(Zn)Te and Cd(Mn)Te, is also observed in our ingots. Such behavior can be explained by migration of impurities from the molten Te inclusions to the crystal bulk.

REFERENCES

[1] Beckett, D. J. S., Bernard, P., Lamarche, G. and Woolley, J. C., "Growth of Bulk Single Crystals of Cd,Zn,Mn,Te Alloys," J. Solid State Chem. 73, 585-587 (1988).

[2] Hwang, Y., Kim, H., Cho, S., Um, Y., Park, H., Jeen, G., "Temperature dependence of the Faraday rotation in diluted magnetic semiconductors $Cd_{1-x-y}Mn_xZn_yTe$ crystals," J. Magn. Mater. 304, e312–e314 (2006).

[3] Hwang, Y., Chung, S., Um, Y., "Weak ferromagnetism in CdMnZnTe single crystal," PSS (C) 4(12), 4457–4460 (2007).

[4] Chou, W.C., Chen, F.R., Chiang, T.Y., Shin, H.Y., Sun, C.Y., Lin, C.M., Chern-Yu, K., Tsai, C.T., Chuu, D.S., "Growth and characterization of $Cd_{1-x-y}Zn_xMn_yTe$ crystals," J. Cryst. Growth 169, 747-751 (1996).

[5] Kopach, V., Kopach, O., Fochuk, P., Shcherbak, L., Bolotnikov, A. E. and James, R. B., "Differential thermal analyses of $Cd_{0.95-x}Mn_xZn_{0.05}Te$ alloys," Proc. SPIE 8852, 88521D-1-5 (2013).

[6] Kopach, V., Kopach, O., Fochuk, P., Shcherbak, L., Bolotnikov, A. E. and James, R. B., "Kinetic parameters of $Cd_{1-x-y}Mn_xZn_yTe$ alloys melting and crystallization processes," PSS (C) 11, 1533-1537 (2014).

[7] Kopach, V., Kopach, O., Fochuk, P., Filonenko, S., Shcherbak, L., Bolotnikov, A. E. and James, R. B., "Vertical Bridgman growth and characterization of $Cd_{0.95-x}Mn_xZn_{0.05}Te$ (x=0.20, 0.30) single-crystal ingots," Proc. SPIE 10392, 1039214-1-8 (2017).

[8] Fochuk, P., Nykonyuk, Ye., Verzhak, Ye., Kopach, O., Panchuk, O., Bolotnikov, A. E., James, R. B., "Dopant Content and Thermal Treatment of $Cd_{1-x}Zn_xTe$<In>: Effects on Point-Defect Structures," IEEE Trans. Nucl. Sci. 56 (4), 1784-1790 (2009).

[9] Zhang, J., Jie, W., Wang, T., Zeng, D., Hao, Y., He, K., "Vertical Bridgman growth and characterization of CdMnTe substrates for HgCdTe epitaxy," J. Cryst. Growth 310, 3203-3207 (2008).

[10] Zhang, J., Jie, W., Wang, L. and Luan, L., "Twins in CdMnTe single crystals grown by Bridgman method," Cryst. Res. Technol 45, 7-12 (2010).

[11] Fochuk, P., Nakonechnyi, I., Panchuk, O., Kopach, O., Nykonyuk, Y., Grill, R., Belas, E., Kim, K. H., Bolotnikov, A. E., Yang, G., James R. B., "Changes in the Electrical Parameters of CdTe-based Crystals During Isothermal Annealing," IEEE Trans. Nucl. Sci. 62(3), 1239-1243 (2015).

[12] Fochuk, P., Nakonechnyi, I., Kopach, O., Verzhak, Ye., Panchuk, O., Komar, V., Terzin, I., Kutnij, V., Rybka, A., Nykoniuk, Ye., Bolotnikov, A. E., Camarda, G. C., Cui, Y., Hossain, A., Kim, K. H., Yang, G., James, R. B., "High-temperature treatment of In-doped CZT crystals grown by the high-pressure Bridgman method," Proc. SPIE 8507, 85071L-850711L (2012).